1-1-2018

Origin of magnetic flux-jumps in Nb films subject to mechanical vibrations and corresponding magnetic perturbations

Igor A. Golovchanskiy
University of Wollongong, ig684@uowmail.edu.au

Alexey V. Pan
University of Wollongong, pan@uow.edu.au

Tom H. Johansen
University of Wollongong, tomjo@uow.edu.au

Jonathan George
University of Wollongong, jgg824@uowmail.edu.au

Igor Rudnev
Moscow Engineering Physics Institute

See next page for additional authors

Origin of magnetic flux-jumps in Nb films subject to mechanical vibrations and corresponding magnetic perturbations

Abstract

In this paper the origin of flux-jumps in Nb thin films is established during magnetization measurements using a vibrating sample magnetometer (VSM). Magnetization measurements of the flux avalanche activity show its strong dependence on frequency and amplitude of VSM vibration. In particular, under certain conditions the vibrations induce a transition from a stable superconducting critical state to an undercritical state, accompanied by the 20-fold drop in the magnetic moment. These features allow the elucidation of the origin of the flux-jumps. In contrast to the commonly assumed thermomagnetic instabilities to be responsible for the flux-jumps in Nb films, our results provide solid support for an alternative explanation being due to criticality-built instability well represented by a sandpile. Considering properties of the flux-flow during a flux avalanche regime allows us to estimate nonuniformity of a magnetic field in a VSM sample space developed as a result of vibrations.

Disciplines

Engineering | Physical Sciences and Mathematics

Publication Details

Authors

Igor A. Golovchanskiy, Alexey V. Pan, Tom H. Johansen, Jonathan George, Igor Rudnev, Anatoly B. Rosenfeld, and Sergey Fedoseev

Origin of magnetic flux-jumps in Nb films subject to mechanical vibrations and corresponding magnetic perturbations

Igor A. Golovchanskiy,[1,2,3] Alexey V. Pan,[1,4,*] Tom H. Johansen,[1,5] Jonathan George,[1] Igor A. Rudnev,[4] Anatoly Rosenfeld,[6] and Sergey A. Fedoseev[1,6]

[1]*Institute for Superconducting and Electronic Materials, University of Wollongong, Northfields Avenue, Wollongong, New South Wales 2522, Australia*

[2]*Moscow Institute of Physics and Technology, State University, 9 Institutskiy pereulok, Dolgoprudny, Moscow Region 141700, Russian Federation*

[3]*National University of Science and Technology (MISIS), 4 Leninsky prospekt, Moscow 119049, Russian Federation*

[4]*National Research Nuclear University MEPhI (Moscow Engineering Physics Institute), 31 Kashirskoye Shosse, 115409 Moscow, Russian Federation*

[5]*Department of Physics, University of Oslo, Blindern, N-0316 Oslo, Norway*

[6]*Centre for Medical Radiation Physics, University of Wollongong, Northfields Avenue, Wollongong, New South Wales 2522, Australia*

In this paper the origin of flux-jumps in Nb thin films is established during magnetization measurements using a vibrating sample magnetometer (VSM). Magnetization measurements of the flux avalanche activity show its strong dependence on frequency and amplitude of VSM vibration. In particular, under certain conditions the vibrations induce a transition from a stable superconducting critical state to an undercritical state, accompanied by the 20-fold drop in the magnetic moment. These features allow the elucidation of the origin of the flux-jumps. In contrast to the commonly assumed thermomagnetic instabilities to be responsible for the flux-jumps in Nb films, our results provide solid support for an alternative explanation being due to criticality-built instability well represented by a sandpile. Considering properties of the flux-flow during a flux avalanche regime allows us to estimate nonuniformity of a magnetic field in a VSM sample space developed as a result of vibrations.

I. INTRODUCTION

Large jumps in magnetization, temperature, ultrasonic attenuation, and resistivity have been observed in many superconducting materials since the early 1960s [1–3]. In general, the phenomenon of magnetic instability is associated with a transition of superconductors into an undercritical state after magnetic flux floods the sample in an uncontrolled avalanchelike fashion. These flux avalanche events often result in catastrophic consequences in practical applications due to significantly suppressed critical current and/or magnetization.

Two types of magnetic instability are usually considered. One type is the thermo-magnetic instability (TMI). The TMI is induced by a positive feedback between moving flux and the associated Joule heating, coupled by a highly nonlinear voltage-current characteristic of the superconductor [1]. A comprehensive description of TMI flux avalanches is provided by analyzing how perturbations to the critical state evolve according to the thermal diffusion and Maxwell equations [4–7].

An alternative type of avalanche mechanism is self-organized criticality (SOC). SOC occurs in dynamical systems with extended spatial degrees of freedom with a pile of sand being a most common example [8–10]. Within SOC a system of superconducting vortices, driven slowly by sweeping the applied magnetic field, naturally organizes itself into a self-organized metastable state through scale-invariant avalanches. The SOC avalanches have a robust power-law size distribution $P(s) \sim s^{-\tau}$, where s is the size of the avalanche [2]. The value of the critical exponent τ is universal in the sense that it should be robust to changes in the system. Pure SOC does not consider the thermal nature of the instability for systems with minimum amounts of static disorder (i.e., pinning) [11]. Yet, although a thermal runaway never occurs in SOC systems, thermal fluctuations induced by dissipative vortex propagation may affect the critical exponent [12,13].

Although, generally, it is believed that the flux avalanches observed in Nb films during magnetization measurements have a TMI nature [14–17], a precise mechanism of these flux avalanches is debatable. At the same time, magneto-optical imaging (MOI) reveals dendrite flux avalanches in superconducting Nb thin films. On one hand, a thermomagnetic nature of dendrite avalanches seems well established [18–25]. On the other hand, signatures of criticality-driven flux avalanches in Nb films [2,11,12,26] and Nb bulk geometries [27] were also explicitly demonstrated. However, it should be noted that experimental conditions during MOI, such as thermal coupling, magnetic-field sweep rate, and range of applied magnetic-fields (B_a), significantly differ from those relevant to magnetization measurements. In addition, certain inconsistencies of the TMI-based description of the flux-jump process in Nb films during magnetization measurements were noted in Ref. [14].

In this paper, we explore the origin of flux-jumps in Nb thin films during magnetization measurements. We show that

certain aspects of the flux-jump phenomenon in a conventional Nb thin-film superconductor are inconsistent with TMI considerations but rather point towards the sandpilelike origin of avalanches.

II. EXPERIMENTAL DETAILS

A Nb film of 450-nm thickness was produced by magnetron sputtering from a N4 purity Nb target on a (5×5)-mm^2 SrTiO$_3$ single-crystal substrate. The back pressure in the deposition chamber was $\sim 10^{-9}$ mBar. The deposition was performed at (6.5×10^{-3})-mBar argon pressure and a 0.6-Å/s deposition rate. During the deposition the substrate temperature was kept at $350\,^{\circ}$C by an infrared heater made from a set of halogen lamps. The obtained Nb thin film has the superconducting critical temperature of $T_c = 8.4 \pm 0.1$ K, which was measured by a Quantum Design magnetic property measurement system (MPMS) at an out-of-plane magnetic field of 2.5 mT.

This film with relatively low T_c was specifically selected for this paper. The flux avalanche process in Nb films with lower T_c has been observed at substantially higher applied magnetic fields than in films with high $T_c \simeq 9$ K (see Figs. 2 and 3 in Ref. [28], or MgB$_2$ bulk [41]). The observation of flux avalanche activity at higher magnetic fields enables a more detailed investigation of corresponding dependencies on B_a and/or measurement parameters. The measurements were performed at $T = 2.5$–3 K since the range of magnetic fields over which flux avalanches occur rapidly decreases at higher temperatures [14,16,17].

Magnetization measurements were performed by a Quantum Design vibrating sample magnetometer (VSM) physical property measurement system (PPMS) supplied with 14 T superconducting solenoid. The applied magnetic field sweep rate is kept at $dB_a/dt = 5 \times 10^{-3}$ T/s for all the measurements. The magnetic field is applied in the out-of-plane direction. The critical current density is determined from magnetization measurements using the Bean formula for the rectangular samples [29]. Importantly, our measurements are carried out employing various frequencies and amplitudes of the VSM. In previous works [28,30,31], nontrivial effects of vibration on the field dependence of the critical current density [$J_c(B_a)$] have been established for various superconductors. The origin of the effect is due to movements of the samples in the slightly inhomogeneous field of the magnet or/and due to small sample displacements/tilt with respect to the magnet's axis. These cause magnetic perturbations on the vortex matter and lead to additional driving forces inserted on the driven vortex lattice in the superconductors. This results in the degradation of $J_c(B_a)$ and the irreversibility field. The mechanism behind the relaxation of the vortex lattice in a sweeping magnetic field via magnetic perturbations is somewhat similar to the vortex shaking mechanism [32–34]. In this paper, we show that vibration also strongly affects magnetization during flux avalanche activity.

III. EXPERIMENTAL RESULTS

Figure 1 shows hysteresis dependencies of magnetization on an applied magnetic-field [$M(B_a)$] in both ascending and descending fields measured in the field-cooled (FC) state
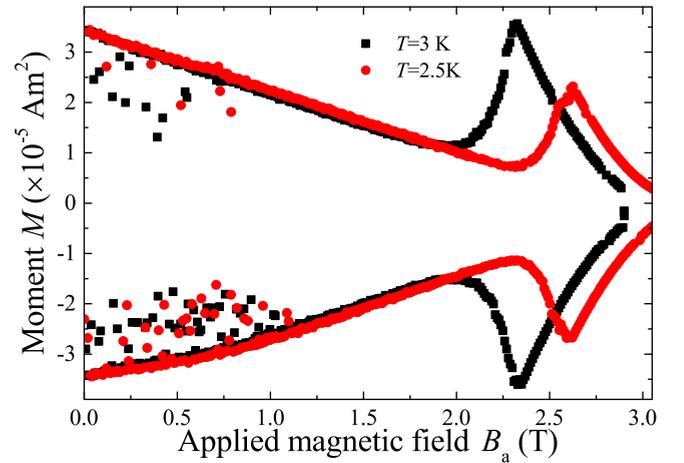

FIG. 1. Dependencies of magnetization on the applied magnetic field measured at standard VSM settings $f = 40$ Hz and $A = 2$ mm.

measured with standard VSM settings for vibrations ($A = 2$ mm, $f = 40$ Hz). The superconducting critical state of the film at higher magnetic fields is well distinguished from the undercritical noisy state at lower fields by abrupt transition of the magnetization with the peak on the $M(B_a)$ curves at $B_a \sim 2.5$ T. These kinds of peaks on $M(B_a)$ are commonly referred to as the second magnetization peaks (SMPs). In our case, they correspond to the onsets of the critical state of the superconductor as discussed in Refs. [14–17,35].

At $B_a < B_{\mathrm{SMP}}$, the film is subjected to multiple flux-jumps. Typically, these flux avalanches are stochastic and locally might form a dendrite pattern during flux propagation [6,26,36]. Although each avalanche event has only local impact and a relatively small effect on total magnetization, they occur frequently, i.e., with very short time and applied magnetic-field intervals. Therefore, they manifest themselves as a strongly suppressed noisy signal in corresponding $M(B_a)$ curves.

Figure 2 shows hysteresis dependencies of magnetization on the applied magnetic-field [$M(B_a)$] in both ascending and descending fields measured in the FC state with different amplitudes (A) and frequencies (f) of vibrations. The noise at $B_a < B_{\mathrm{SMP}}$ was removed. In the critical state (i.e., at $B_a \gtrsim B_{\mathrm{SMP}}$), an increase in f and/or A of the VSM parameters leads to a progressive reduction of $M(B_a)$ (Fig. 2). The smallest VSM settings ($f = 2$ Hz and $A = 1$ mm) correspond to an almost unperturbed regime. More detailed discussions on the impact of the vibrations on the magnetization and critical current of the superconductors in the critical state can be found in Refs. [28,30,31]. In Fig. 2, it is obvious that larger f and/or A promote the general drop in $M(B_a)$ and corresponding M_{SMP} at the SMP as well as larger values of B_{SMP} expanding the magnetic-field region over which flux avalanche instability occurs. In particular, in descending B_a, B_{SMP} increases from $\simeq 2.45$ T for $f = 2$ Hz and $A = 1$ mm to $\simeq 2.65$ T for $f = 40$ Hz and $A = 4$ mm. This evolution of B_{SMP} and M_{SMP} with f and A is illustrated in Fig. 2 with the arrows.

Figure 3 shows a few selected $J_c(B_a)$ dependencies calculated from the corresponding magnetization data measured at different VSM frequencies and amplitudes at 2.5 and 3 K. B_{SMP} can be identified in the $J_c(B_a)$ curves. B_{SMP} is reduced
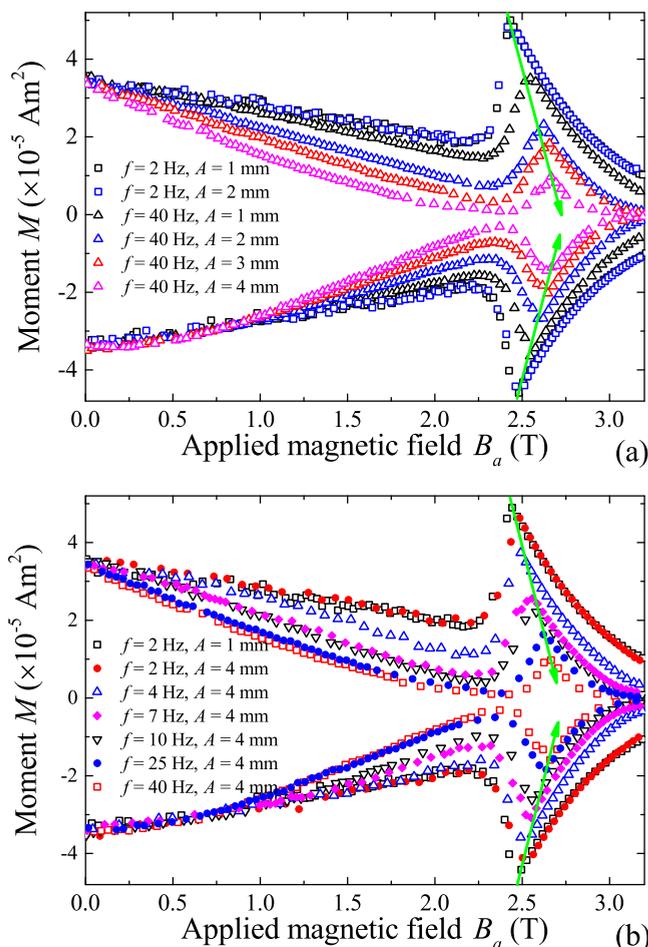
FIG. 2. Dependencies of magnetization on the applied magnetic field measured at (a) $T = 2.5$ K with fixed f and varied A and (b) with fixed A and varied f. Evolutions of B_{SMP} and M_{SMP} with f and A are illustrated with the arrows.

from $\simeq 2.5$ T at $T = 2.5$ K to $B_{SMP} \simeq 2.2$ T at $T = 3$ K for $f = 2$ Hz and $A = 1$ mm. The B_{SMP} dependence on T is well documented in Refs. [14,16,17]. A clear dependence of B_{SMP} on f and A is also obvious. Furthermore, Figs. 2 and 3 indicate a dramatic influence of vibrations on the magnetization and the critical current: at $T = 2.5$ K and $B_a \approx 2.5$ T the change in frequency from 2 to 40 Hz induces a transition from a stable critical state with high M and J_c to the undercritical state with M and J_c reduced by a factor of ~ 20. Such dramatic drops in the magnetization/critical current density induced by vibrations at low frequencies/amplitudes can have catastrophic consequences for applications where such vibrations can naturally appear. In addition, such transitions can obviously undermine the objectiveness of the characterization in thin films. Therefore, understanding the origin of the flux-jumps during VSM magnetization measurements is of crucial importance.

IV. DISCUSSION: ORIGIN OF FLUX-JUMPS IN NB THIN FILMS DURING MAGNETIZATION MEASUREMENTS

A. Inconsistencies of vibration-driven flux-jumps with TMI considerations

First, we assume that the flux avalanche activity in Figs. 2 and 3 is of TMI origin. A key parameter of TMI flux-jumps
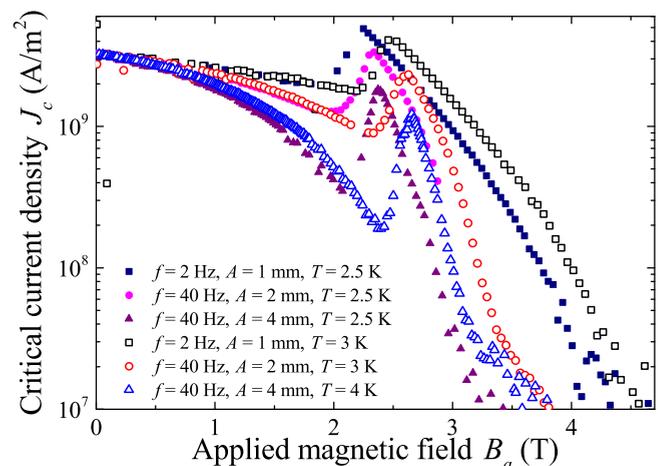

FIG. 3. Selected dependencies of the critical current density on the applied magnetic field measured in the FC state at $T = 2.5$ and 3 K with $dB_a/dt = 5 \times 10^{-3}$ T/s and varied f and A.

is a dimensionless ratio of thermal and magnetic diffusion coefficients [1,4–7],

$$\tau_0 = \mu_0 \kappa \sigma / C, \qquad (1)$$

where κ is the thermal conductivity, σ is the electrical conductivity, and C is the specific heat. Criterion τ_0 separates the adiabatic regime ($\tau_0 < 1$) from the dynamic regime ($\tau_0 > 1$). The adiabatic regime features the rapid propagation of the flux accompanied by the adiabatic heating of the superconductor, i.e., there is not enough time to redistribute and remove the heat released due to the flux motion. The dynamic regime is described by the fixed spatial distribution of the magnetic flux upon the rapid heat propagation.

In the adiabatic regime ($\tau_0 < 1$), a thin-film superconductor develops dendritic flux avalanches due to "fingering" instability within nonlocal electrodynamics [5,7] regardless the heat transfer conditions to the substrate or environment. MOI images of dendritic flux-jumps in Nb can be found in Refs. [37,38]. Thinner films demonstrate higher instability towards dendritic flux-jumps. The nonlocal TMI approach applied for thin films in the adiabatic regime has successfully been verified in a series of works (see Refs. [5,6,39,40]). Nevertheless, as noted by Mints and Brandt [4], for standard VSM magnetization measurements in the Nb superconductor, the ratio τ_0 is extremely large ($\tau_0 \sim 10^5$) mainly due to very high electrical conductivity. The high value of τ_0 can be verified using the following typical characteristics for a Nb film [5,37]: $\kappa(T = 4.2$ K$) \sim 10$ W K^{-1} m^{-1}, $C(T = 4.2$ K$) \sim 10^3$ J K^{-1} m^{-3}, and $\sigma \approx J_c / n E_{cr} \sim 10^{14}$ (Ω m)$^{-1}$, where $E_{cr} \sim 10^{-5}$ V/m [30], $J_c > 10^{10}$ A/m^2 (see Fig. 3) and $n \simeq 30$ is a typical exponent used in power-law relation [7] $E \sim J^n$. Thus, it is unlikely that the flux-jumps observed in Fig. 2 are of the TMI origin.

In a dynamic approximation ($\tau_0 > 1$), uniform flux-jumps dominate. However, the uniform instability can be developed only in the case of poor heat transfer from the superconductor [4,5,7]. This condition can be represented as [7]: $h\tau_0 < 1$, where $h \sim h_0 a^2 / (\kappa d)$ is a dimensionless heat transfer parameter with h_0 being the heat transfer coefficient in Newton's
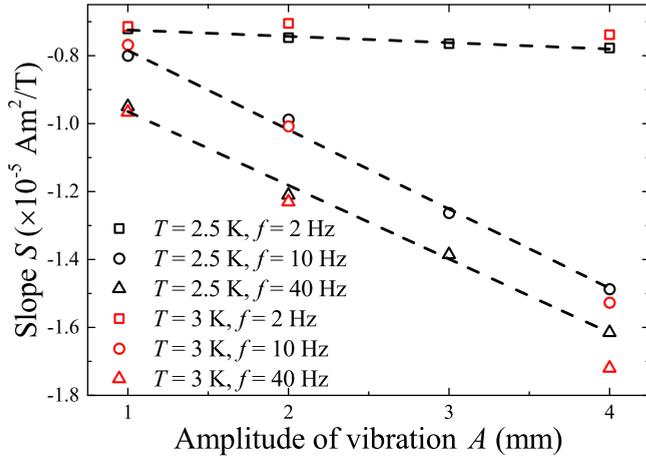
FIG. 4. Dependencies of the slope of $M(B_a)$ on A at varied f. The $M(B_a)$ data are taken at the descending magnetic-field $B_a < 2$ T.

cooling law, $a \sim 10^{-5}$ m being an adiabatic length, and d being the thickness of the film. Thus, a uniform flux-jump in the dynamic regime occurs when the heat transfer coefficient h_0 is sufficiently small or film thickness d is large (for example, in Nb foils [25] or Nb bulk [28], or MgB$_2$ bulk [41]). In our case, we can get $h\tau_0 \gg 1$ with a reasonable heat coupling of the film to the substrate (a heat transfer coefficient $h_0 \sim 10^3$ W m^{-2} K^{-1}) [6,25]), a *thin* film with $d = 450$ nm and high $\tau_0 \gg 1$, which makes our thin Nb film stable for the uniform flux-jump. Thus, according to the TMI criteria, the Nb thin film should be completely stable against the flux-jumps during VSM magnetization measurements.

Second, we provide some phenomenological arguments against the TMI origin of the flux-jumps below. Within the TMI approach, superconductors with smaller J_c are more stable against flux-jumps. Indeed, the enhanced stability was shown in samples with smaller J_c, exhibiting the reduced B_{SMP} [39]. In our previous works [28,30,31], we have demonstrated that the vibration of the superconductor in the critical state suppresses the efficiency of vortex pinning and considerably reduces $J_c(B_a)$. It is also evident in Fig. 3 at $B_a > B_{SMP}$. Hence, within the TMI considerations one would expect a reduction of B_{SMP} if f and/or A were increased. Yet, a completely opposite trend is observed in Figs. 2 and 3.

Third, the dynamics of the TMI avalanches is temperature dependent. Both the size [5] and the speed [36] of each individual TMI avalanche reduce at higher T due to smaller J_c [5,39] or reduced thermal gradients [42]. Smaller/slower avalanche events reduce the avalanche activity and result in smaller drops of $M(B_a)$ at $B_a < B_{SMP}$ (e.g., Ref. [18]). Since the magnetic field is swept continuously the general avalanche dynamics, i.e., its speed, size, and frequency, may be characterized by the slope of approximately linear $M(B_a)$ dependence at B_a well below B_{SMP}. Figure 4 shows the dependencies of the $M(B_a)$ slope in a descending magnetic field on A for different f's at $T = 2.5$ and 3 K in $B_a < 2$ T, which is well below B_{SMP}. Figure 4 demonstrates that the slope of $M(B_a)$ in the flux-jump regime is determined by the VSM settings only and does not depend on T despite a significant difference in the critical current density at these

two temperatures (Fig. 3) and likely the associated difference in the thermal instability. Therefore, Fig. 4 indicates that the dynamics of the flux avalanche process is temperature independent, which contradicts expectations from TMI. The fact that $M(B_a)$ is independent of T at $B_a < B_{SMP}$ is also shown in Refs. [16,17] as well as in Fig. 3 for curves measured with the same f and A but at different T's. Note, unlike the dynamics of the flux avalanche process, the transition field from the avalanche state to the critical state B_{SMP} is strongly temperature dependent.

Finally, to make the overall picture complete, we note that the TMI models are the most successful in describing instabilities in low applied magnetic fields with the first avalanches occurring in partially penetrated samples. MOI often employed for evidencing the TMI origin is usually performed at relatively low magnetic fields, and its sample environment is drastically different from magnetization measurements: A sample is placed on a large block of brass and covered with a magneto-optical indicator film [43], whereas the magnetization measurements are performed with a sample attached to a hollow straw by a tiny piece of a sticky tape (or something similar). Some TMI models diverge if the applied magnetic field approaches the field of the full magnetic flux penetration in the superconductor [6,39]. The full penetration occurs typically at $B_a \lesssim 0.1$ T. In the present paper, the Nb thin film demonstrates flux avalanches in magnetic fields up to $B_a \lesssim 2.5$ T upon magnetization measurements (Fig. 2), which is far above the full penetration field.

Thus, the TMI criteria [Eq. (1)], the dependence of B_{SMP} on J_c, and the other results obtained for the dynamics of the flux-jump instability upon the measurements of $M(B_a)$ in Nb thin films with different frequencies and amplitudes of VSM firmly advocate against the TMI origin of flux-jumps.

B. SOC considerations for vibration-driven flux-jumps

An alternative mechanism proposed for the flux-jumps is governed by criticality-built instabilities. In particular, the flux avalanche process in superconducting Nb driven by SOC was observed in several works [2,11,12,26,27]. In SOC, a vortex system driven slowly by sweeping the magnetic field organizes itself into a metastable state through scale-invariant avalanches, which have robust statistics.

The mechanism of criticality-driven flux-jumps can simply be represented by a dynamics of sand in a pile. Since it does not consider thermal runaway, the dynamics of flux-jumps is independent of temperature as demonstrated in Fig. 4. Moreover, avalanche dynamics in sand considers a certain response to mechanical vibration. Horizontal or vertical vibrations of a pile imposes additional alternating forces acting on grains, which effectively assist to "depin" and propagate grains decreasing the critical slope of the pile [44–49]. The critical slope is progressively decreased with the larger amplitude and/or frequency of the mechanical vibrations.

Small vibrations of a superconductor in a slightly inhomogeneous applied magnetic field create small alternating currents. Alternatively, such alternating currents are induced if the vibrations are not perfect and involve any kind of tilting. These currents would depin and propagate the magnetic flux

within the superconductor [28,30,31], qualitatively similar to alternating accelerations in sandpiles.

Thus, the dynamics of flux avalanches and, in particular, its response to vibration demonstrated in Figs. 2–4 are expected to reveal considerable similarities with the dynamics of sandpiles. Taking into account the vast inconsistencies with the TMI origin discussed in the previous section, these similarities would indicate that the criticality-built instability is the origin for the flux-jumps in Nb films.

C. Phenomenological model for flux-jumps in Nb films

In terms of sandpile dynamics, the gradient of the magnetic flux in the Nb thin-film sample is continuously mobilized upon magnetization experiments via a constant magnetic field sweep rate [47]. Macroscopically, it indicates a conventional vortex creep (flux creep) regime combined with more substantial movement upon flux avalanches. As the flux moves, the Lorentz force, established by the gradient of magnetic flux and represented by M, is balanced by the friction force working on the moving vortices. This friction force provides a simple dependence of magnetization on the velocity of *all moving* vortices,

$$M(B_a) = \eta(B_a)V(B_a), \tag{2}$$

where $V(B_a) = \frac{l}{2}\frac{dB_a}{dt}/B_a$ is the field-dependent velocity of vortices in the VSM experiments [30]. Note, the velocity of the vortex propagation $V(B_a)$ is essentially controlled by the constant magnetic-field sweep rate dB_a/dt at both the critical state and the flux-jump regime, which is one of the key points for the phenomenological model we propose. Here, $l = 0.005$ m being the transverse size of the film, $dB_a/dt = 5 \times 10^{-3}$ T/s, and $\eta(B_a)$ is an effective field-dependent coefficient of vortex friction. Note, this friction coefficient includes both vortex pinning and Bardeen-Stephen viscosity [50,51]. At the same time, the vibration assists in propagating the vortices and reducing the magnetic flux gradient (i.e., M), hence the vibration effectively reduces the coefficient of vortex friction η. Below, we construct the dependence of η on B_a, f, and A using general arguments.

Figure 5 shows experimental $M(B_a)$ dependencies at $B_a < B_{SMP}$ averaged over ascending and descending fields taken from Fig. 2. The $M(B_a)$ curves in Fig. 5 reflect the general effect of vibration on η as follows. Taking into account Eq. (2), it is obvious that η decreases linearly as a function with A at high B_a, i.e., $\eta \sim \alpha A$ [see the insets for Figs. 5(a) and 4]. According to Figs. 4 and 5(b) the dependence of η on f is somewhat more complex, leveling at $f_0 \gtrsim 35$ Hz [see the inset to Fig. 5(b)]. This leveling corresponds to bunching up $M(B_a)$ dependencies in Figs. 2(b) and 5(b). Similar dependencies of $M(B_a), J_c(B_a)$ on f exhibiting the bunching at higher frequencies were observed and discussed for yttrium barium copper oxide (YBCO) thin films in the critical state in Refs. [28,30].

Now, we assume that η is an averaged characteristic over a single period of the VSM vibration, i.e., η is proportional to some effective frequency ($\eta \propto f_{eff}$). The same situation would be with the average velocity $\bar{V}$ of the vortex propagation over a single period of the VSM vibration. Since in the VSM experiment $V(t) \sim 1/t$, the average velocity over the period of vibration $1/f$ takes the form
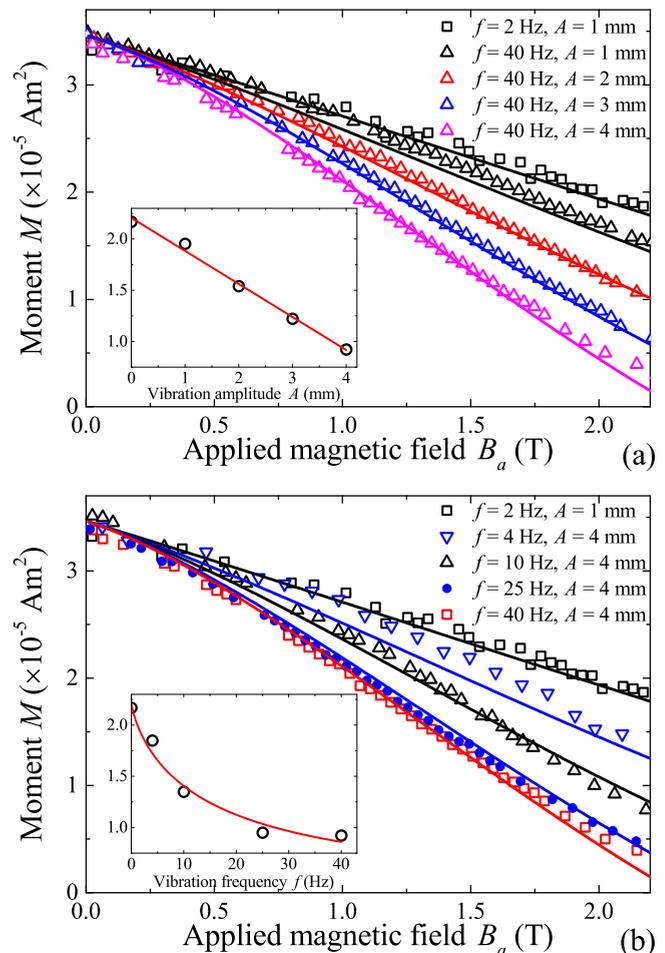

FIG. 5. $M_{fj}(B_a)$ dependencies averaged over ascending and descending field branches of the magnetic moment, measured with (a) different amplitudes at $f = 40$ Hz and (b) different frequencies at $A = 4$ mm. The solid lines in the main panels show the fit by Eq. (2) with the coefficient of viscosity determined by Eq. (3) and corresponding with the VSM settings for f and A. The insets show the dependence of the magnetic moment of the flux-jump region measured at 1.75 T (a) on A at $f = 40$ Hz and on f at $A = 4$ mm. The solid lines in the insets show (a) the linear fit to $M_{fj}(A)$ and (b) the fit of $M(f) \propto -f \ln(1 + 35/f)$ to $M_{fj}(f)$. See the text for the details.

$$\bar{V}(t) \sim f \int_t^{t+1/f} V(t)dt \sim f \int_t^{t+1/f} \frac{1}{t}dt = f \ln(1 + 1/tf).$$ Therefore, we presume that $f_{eff} = f \ln(1 + f_0/f)$, where f_0 is a free parameter, which denotes the frequency where $M(B_a)$ curves start to bunch up.

In addition, η should not depend on the velocity of vortex propagation since there are no reports on the dependence of sandpile dynamics on the rate of sand supply, i.e., $\eta \sim 1/V(B_a)$. Finally, η should have a nonlinear dependence on B_a in order to conform to a distinctive curvature of $M(B_a)$ at $B_a < 0.7$ T measured with $f > 2$ Hz and/or A in Fig. 5, e.g., $\propto B_a^x/V(B_a)$.

Multiplying all the factors considered above, we obtain the expression for the effective friction coefficient η,

$$\eta = \eta_0[1 - \alpha A B_a^x f \ln(1 + f_0/f)/V(B_a)], \tag{3}$$

where x is a free fitting parameter, so as α, which includes all necessary units and defines the degree of M reduction by vibration in Fig. 5.

Note, the factor $\delta = (\alpha A B_a^x)$ in Eq. (3) can be interpreted as the distance of the additional propagation of vortices induced by vibration over one effective period $1/f_{\text{eff}}$. The entire expression $\alpha A B_a^x f \ln(1 + f_0/f)$ can be understood as the additional velocity of vortex propagation induced on vortices, propagating with the base speed $V(B_a)$ under constant B_a. The B_a^x dependence appears only due to the perturbations arising due to the vibrations.

In addition, the ratio $f/V(B_a)$, which appears in Eq. (3), replicates the scaling of the effect of vibration with frequency f and the magnetic-field sweep rate arising due to the additional vortex motion inserted by the vibrations and associated energy dissipations. This scaling was considered for J_c and the irreversibility field of YBCO thin films in Ref. [28].

The solid lines in Fig. 5 are the fits of Eqs. (2) and (3) to the $M(B_a)$ data with the following fitting parameters:

$\eta_0 \simeq 0.035$ A m s, $\alpha \simeq 2.9 \times 10^{-8}$ m/mm, $x \simeq 0.75$, and $f_0 \simeq 35$ Hz.

The expression for the distance of vibration-induced propagation $\delta = (\alpha A B_a^{0.75})$ allows us to estimate the nonuniformity of the magnetic field in a sample space during vibration as follows. Vortices at the edge of the sample need to travel an additional distance in order to keep the uniform flux distribution. For example, at $B_a = 1$ T for $A = 4$ mm $\delta \simeq 1.2 \times 10^{-7}$ m, which results in the nonuniformity of the magnetic field of $\sim \delta/(l/2) \sim 5 \times 10^{-5}$. This estimation is well consistent with previous estimations of nonuniformity of the magnetic fields in MPMS sample space [52,53], which can induce the so-called paramagnetic Meissner effect [52,54].

It is important to note that the phenomenological approach [Eqs. (2) and (3)] is valid only below B_{SMP}. At $B_a > B_{\text{SMP}}$ the conventional critical state model is applicable.

V. SUMMARY

In this paper, the origin of flux-jumps in Nb thin films during magnetization measurements is studied employing a VSM magnetometer. It is shown (Figs. 2 and 3) that the magnetization and critical current measured during flux avalanche activity are extremely sensitive to the VSM vibration: higher f and/or A promote the additional reduction of magnetization

during flux avalanche activity. The maximum drop in $M(B_a)$ by a factor of 20 is obtained between the magnetizations measured at $f = 2$ Hz, $A = 1$ mm, and $f = 40$ Hz, $A = 4$ mm for $B_a \simeq 2.4$ T. This drop is the vibration-induced transition from a stable critical state with high M and J_c to the undercritical state arising due to flux-jumps.

Although it is commonly assumed that flux-jumps in Nb films occur due to thermomagnetic instability, we show that TMI-based considerations are inapplicable. Our results point out towards the alternative model of self-organized criticality (analogous to sandpile dynamics) responsible for the instability origin. Considering a flux motion macroscopically [Eq. (2)], we derived the expression for magnetization dependence on B_a, f, and A at $B_a < B_{\text{SMP}}$ [Eq. (5)]. This expression is built considering the effect of vibrations on the effective coefficient of vortex friction. Analyzing the $M(B_a)$ curves measured with different frequencies and amplitudes of VSM has allowed us to estimate a nonuniformity of the magnetic field in a sample space ($\sim 10^{-5}$) which is comparable with the other available estimations in the literature.

In conclusion, we should note that within a criticality-built instability the nature of B_{SMP} may need to be revisited. In the TMI approach, B_{SMP} signifies a transition from the thermally unstable regime of flux-jumps to the thermally stable critical state. In SOC, B_{SMP} may identify some characteristic velocity of vortex propagation. At lower fields where the velocity of vortices is high, the motion of vortices is guided by the criticality-driven mobilization. Once the velocity becomes lower than the characteristic one, i.e., at fields higher than the B_{SMP}, the motion of the vortices transits to vortex creep-driven propagation, which is typical for the superconducting critical state.

[1] R. G. Mints and A. L. Rakhmanov, Rev. Mod. Phys. **53**, 551 (1981).

[2] E. Altshuler and T. H. Johansen, Rev. Mod. Phys. **76**, 471 (2004).

[3] M. R. Wertheimer and J. le G. Gilchrist, J. Phys. Chem. Solids **28**, 2509 (1967).

[4] R. G. Mints and E. H. Brandt, Phys. Rev. B **54**, 12421 (1996).

[5] I. S. Aranson, A. Gurevich, M. S. Welling, R. J. Wijngaarden, V. K. Vlasko-Vlasov, V. M. Vinokur, and U. Welp, Phys. Rev. Lett. **94**, 037002 (2005).

[6] D. V. Denisov, D. V. Shantsev, Y. M. Galperin, E.-M. Choi, H.-S. Lee, S.-I. Lee, A. V. Bobyl, P. E. Goa, A. A. F. Olsen, and T. H. Johansen, Phys. Rev. Lett. **97**, 077002 (2006).

[7] D. V. Denisov, A. L. Rakhmanov, D. V. Shantsev, Y. M. Galperin, and T. H. Johansen, Phys. Rev. B **73**, 014512 (2006).

[8] P. Bak, C. Tang, and K. Wiesenfeld, Phys. Rev. Lett. **59**, 381 (1987).

[9] P. Bak, C. Tang, and K. Wiesenfeld, Phys. Rev. A **38**, 364 (1988).

[10] M. Paczuski and S. Boettcher, Phys. Rev. Lett. **77**, 111 (1996).

[11] R. J. Wijngaarden, M. S. Welling, C. M. Aegerter, and M. Menghini, Eur. Phys. J. B **50**, 117 (2006).

[12] E. R. Nowak, O. W. Taylor, L. Liu, H. M. Jaeger, and T. I. Selinder, Phys. Rev. B **55**, 11702 (1997).

[13] R. Surdeanu, R. J. Wijngaarden, E. Visser, J. M. Huijbregtse, J. H. Rector, B. Dam, and R. Griessen, Phys. Rev. Lett. **83**, 2054 (1999).

[14] P. Esquinazi, A. Setzer, D. Fuchs, Y. Kopelevich, E. Zeldov, and C. Assmann, Phys. Rev. B **60**, 12454 (1999).

[15] Y. Kopelevich and P. Esquinazi, J. Low Temp. Phys. **113**, 1 (1998).

[16] D. Stamopoulos, A. Speliotis, and D. Niarchos, Supercond. Sci. Technol. **17**, 1261 (2004).

[17] D. Stamopoulos and D. Niarchos, Physica C **417**, 69 (2004).

[18] J. I. Vestgarden, D. V. Shantsev, Y. M. Galperin, and T. H. Johansen, Phys. Rev. B **84**, 054537 (2011).

[19] D. V. Shantsev, P. E. Goa, F. L. Barkov, T. H. Johansen, W. N. Kang, and S. I. Lee, Supercond. Sci. Technol. **16**, 566 (2003).

[20] P. Leiderer, J. Boneberg, P. Brüll, V. Bujok, and S. Herminghaus, Phys. Rev. Lett. **71**, 2646 (1993).

[21] T. Johansen, M. Baziljevich, D. V. Shantsev, P. E. Goa, Y. M. Galperin, W. N. Kang, H. J. Kim, E. M. Choi, M.-S. Kim, and S. I. Lee, Europhys. Lett. **59**, 599 (2002).

[22] A. V. Bobyl, D. V. Shantsev, T. H. Johansen, W. N. Kang, H. J. Kim, E. M. Choi, and S. I. Lee, Appl. Phys. Lett. **80**, 4588 (2002).

[23] U. Bolz, B. Biehler, D. Schmidt, B.-U. Runge, and P. Leiderer, Europhys. Lett. **64**, 517 (2003).

[24] U. Bolz, D. Schmidt, B. Biehler, B.-U. Runge, R. Mints, K. Numssen, H. Kinder, and P. Leiderer, Physica C **388-389**, 715 (2003).

[25] R. Prozorov, D. V. Shantsev, and R. G. Mints, Phys. Rev. B **74**, 220511 (2006).

[26] E. Altshuler, T. H. Johansen, Y. Paltiel, P. Jin, K. E. Bassler, O. Ramos, Q. Y. Chen, G. F. Reiter, E. Zeldov, and C. W. Chu, Phys. Rev. B **70**, 140505 (2004).

[27] S. Field, J. Witt, F. Nori, and X. Ling, Phys. Rev. Lett. **74**, 1206 (1995).

[28] I. A. Golovchanskiy, A. V. Pan, J. George, F. S. Wells, S. A. Fedoseev, and A. Rozenfeld, Supercond. Sci. Technol. **29**, 075002 (2016).

[29] D.-X. Chen and R. B. Goldfarb, J. Appl. Phys. **66**, 2489 (1989).

[30] I. A. Golovchanskiy, A. V. Pan, O. V. Shcherbakova, and S. A. Fedoseev, J. Appl. Phys. **114**, 163910 (2013).

[31] A. V. Pan, I. A. Golovchanskiy, and S. A. Fedoseev, Europhys. Lett. **103**, 17006 (2013).

[32] E. H. Brandt, Phys. Rev. B **48**, 6699 (1993).

[33] E. H. Brandt and G. P. Mikitik, Phys. Rev. Lett. **89**, 027002 (2002).

[34] G. P. Mikitik and E. H. Brandt, Phys. Rev. B **69**, 134521 (2004).

[35] P. Esquinazi, R. Höhne, Y. Kopelevich, A. V. Pan, and M. Ziese, *Physics and Materials Science of Vortex States, Flux Pinning and Dynamics*, edited by R. Kossowsky, S. Bose, V. Pan, and Z. Durusoy, NATO Science Series E Vol. 356 (Kluwer, Dordrecht, 1999), p. 149.

[36] B. Biehler, B. U. Runge, P. Leiderer, and R. G. Mints, Phys. Rev. B **72**, 024532 (2005).

[37] C. A. Durán, P. L. Gammel, R. E. Miller, and D. J. Bishop, Phys. Rev. B **52**, 75 (1995).

[38] M. S. Welling, R. J. Westerwaal, W. Lohstroh, and R. J. Wijngaarden, Physica C **411**, 11 (2004).

[39] V. V. Yurchenko, D. V. Shantsev, T. H. Johansen, M. R. Nevala, I. J. Maasilta, K. Senapati, and R. C. Budhani, Phys. Rev. B **76**, 092504 (2007).

[40] J. Albrecht, A. T. Matveev, J. Strempfer, H.-U. Habermeier, D. V. Shantsev, Y. M. Galperin, and T. H. Johansen, Phys. Rev. Lett. **98**, 117001 (2007).

[41] V. Chabanenko, R. Puźniak, A. Nabiałek, S. Vasiliev, V. Rusakov, L. Huanqian, R. Szymczak, H. Szymczak, J. Jun, J. Karpiński *et al.*, J. Low Temp. Phys. **130**, 175 (2003).

[42] D. V. Shantsev, A. V. Bobyl, Y. M. Galperin, T. H. Johansen, and S. I. Lee, Phys. Rev. B **72**, 024541 (2005).

[43] F. S. Wells, A. V. Pan, S. Wilson, I. A. Golovchanskiy, S. A. Fedoseev, and A. Rozenfeld, Supercond. Sci. Technol. **29**, 035014 (2016).

[44] H. M. Jaeger, C. H. Liu, and S. R. Nagel, Phys. Rev. Lett. **62**, 40 (1989).

[45] M. E. Vavrek and G. W. Baxter, Phys. Rev. E **50**, 3353(R) (1994).

[46] A. A. Aerov, N. S. Vinogradov, and Y. N. Markov, *Proceedings of the XI Session of the Russian Acoustical Society (RAO-XI), Moscow, 2001* (Russian Acoustical Society, Moscow, 2001), p. 339.

[47] D. Rubin, N. Goldenson, and G. A. Voth, Phys. Rev. E **74**, 051307 (2006).

[48] D. L. Amon, T. Niculescu, and B. C. Utter, Phys. Rev. E **88**, 012203 (2013).

[49] F. Zhang, L. Wang, C. Liu, P. Wu, and S. Zhan, Phys. Lett. A **378**, 1303 (2014).

[50] J. Bardeen and M. J. Stephen, Phys. Rev. **140**, A1197 (1965).

[51] Y. B. Kim, C. F. Hempstrad, and A. R. Strnad, Phys. Rev. **139**, A1163 (1965).

[52] D. A. Luzhbin, A. V. Pan, V. A. Komashko, V. S. Flis, V. M. Pan, S. X. Dou, and P. Esquinazi, Phys. Rev. B **69**, 024506 (2004).

[53] A. Schilling, H. R. Ott, and T. Wolf, Phys. Rev. B **46**, 14253 (1992).

[54] F. J. Blunt, A. R. Perry, A. M.Campbell, and R. S. Siu, Physica C **175**, 539 (1991).